Polymer induced depletion potentials in polymer-colloid mixtures

A. A. Louis
Department of Chemistry, Lensfield Road, Cambridge CB2 1EW, United Kingdom

P. G. Bolhuis and E. J. Meijer
Department of Chemical Engineering, University of Amsterdam, Nieuwe Achtergracht 166,
NL-1018 WV Amsterdam, The Netherlands

J. P. Hansen
Department of Chemistry, Lensfield Road, Cambridge CB2 1EW, United Kingdom

The depletion interactions between two colloidal plates or between two colloidal spheres, induced by interacting polymers in a good solvent, are calculated theoretically and by computer simulations. A simple analytical theory is shown to be quantitatively accurate for the case of two plates. A related depletion potential is derived for two spheres; it also agrees very well with direct computer simulations. Theories based on ideal polymers show important deviations with increasing polymer concentration: They overestimate the range of the depletion potential between two plates or two spheres at all densities, with the largest relative change occurring in the dilute regime. They underestimate the well depth at contact for the case of two plates, but overestimate it for two spheres. Depletion potentials are also calculated using a coarse graining approach which represents the polymers as "soft colloids;" good agreement is found in the dilute regime. Finally, the effect of the polymers on colloid–colloid osmotic virial coefficients is related to phase behavior of polymer–colloid mixtures. © 2002 American Institute of Physics. [DOI: 10.1063/1.1483299]

I. INTRODUCTION

Effective potentials are a key to unlocking the equilibrium behavior of many soft-matter systems.[1,2] The basic philosophy behind this coarse-graining approach is that the initial effort in deriving these potentials is recouped when they are input into the well oiled machinery of liquid state theory,[3] or when they are used in computer simulations.[4] An archetypal example is the depletion potential, induced between colloidal particles by nonadsorbing polymers. Asakura and Oosawa[5] first showed that a bath of such polymers, characterized by their radius of gyration R_g, induces an attractive depletion interaction of range $D \approx 2R_g$ between two plates. Their calculation was exact for noninteracting polymers. Later, the same authors, and independently Vrij,[6] derived a depletion potential between two colloidal hard spheres (HS) by approximating the (ideal) polymers as penetrable spheres. This is often termed the Asakura–Oosawa (AO) model.

A good example of the effective potential coarse-graining approach is the calculation of the phase behavior of polymer–colloid mixtures by Gast, Hall, and Russel,[7] and also by Lekkerkerker *et al.*[8] and Meijer and Frenkel.[30] They found, using an AO depletion potential approach, that the fluid–fluid phase line of colloids of radius R_c becomes metastable with respect to the fluid–solid phase line if the size ratio $q = R_g / R_c$ is less than about 0.35, in qualitative agreement with experiments.[9,10] Their work demonstrates how an accurate knowledge of the depletion potential can lead to a good understanding of the equilibrium behavior of colloid polymer mixtures. The latter are important not only because of their relevance to many industrial and biological processes, but also because they form an important model system for equilibrium and nonequilibrium behavior in soft matter science.

Whereas the depletion interaction for ideal polymers is now quantitatively understood, the understanding of the depletion interaction induced by polymers with excluded volume interactions is at best qualitative. Experiments on the phase behavior[9,10] and structure[11,12] of polymer–colloid mixtures also show deviations from the simple AO model,[13,14] as do direct measurements of the depletion potentials.[15–17] Theoretical attempts to directly calculate the depletion potentials for interacting polymers include scaling theory,[18] self-consistent field theory,[19] perturbation theory,[20,21] direct simulations,[22] RG theory,[23,24] as well an interesting new "overlap approximation" method.[25] All these approaches show significant deviations from ideal polymer behavior, but many questions still remain. This is in contrast to binary HS colloid mixtures, where the deviations from the AO potential can now be quantitatively calculated with density functional theory (DFT),[26–28] and the effects of nonideality on the phase behavior are fairly well understood.[29] The goal of our paper is to derive a theory of similar accuracy for the depletion potential induced by interacting polymers in a good solvent.

Before we proceed, an important caveat is that the depletion potential becomes less relevant for phase behavior at larger size ratios q, since many-body interactions become increasingly important.[13,14,30] When $q \gg 1$, i.e., when the colloids are much smaller than the polymers, other approaches, which treat the polymers on a monomer level, are more relevant. Examples include integral equation techniques,[31] scaling theory,[32,33] or renormalization group theory (RG).[34] In

this paper we concentrate on the regime where R_g is of the order of R_c or smaller.

We have recently performed a systematic study of the insertion free-energy of a single colloidal particle in a bath of interacting polymers[35] (henceforth referred to as Paper I), and found important deviations from ideal polymer behavior. In particular, we found that the range of the depletion layer decreases with increasing density ρ, and that this effect is most pronounced in the dilute regime, where $\rho \lesssim \rho^*$; here $\rho^* = \frac{4}{3}\pi R_g^3$ is the overlap density. In the semidilute regime, where $\rho/\rho^* > 1$, we found that the effects of the interactions could be well described by scaling theory.[33] Since these one-body effects were not well captured by (nonadditive) HS-like models, we do not expect straightforward extensions of the DFT techniques that work so well for binary hard HS mixtures, to also perform well for two-body depletion potentials in polymer–colloid mixtures.

To calculate the depletion potentials, we use a similar approach to that used in Paper I, a combination of scaling theories and computer simulations. Since we found in Paper I that the width of the depletion layer decreases with increasing density, we expect a similar trend for the range of the related depletion potential. Throughout this work we focus on the dilute and semidilute regimes[33,36] of the polymers, where the monomer density c is low enough for detailed monomer–monomer correlations to be unimportant; the melt regime, where c becomes appreciable, will not be treated here. Since our models are all athermal, we set $\beta = 1/(k_B T) = 1$.

The paper is organized as follows: The case of the depletion interaction between two plates is discussed in detail in Sec. II. We show that it is closely related to the problem of determining the surface tension $\gamma_w(\rho)$, which was solved in Paper I. Just as was found for $\gamma_w(\rho)$, the depletion potential simplifies in the semidilute regime. In Sec. III, we discuss the depletion interaction between two spheres. We compare the results of direct Monte Carlo (MC) simulations of the interaction between two HS colloids induced by a bath of self-avoiding walk (SAW) polymers to a potential derived within the Derjaguin approximation.[37] The Derjaguin approximation works much better than one would naively expect because of a cancellation of errors related to the deformation of polymers around a sphere. Using an extension of the Derjaguin approximation, we derive a new semiempirical depletion potential which appears to be nearly quantitative for $q \lesssim 1$, the regime where depletion potentials are most relevant for the phase behavior and structure of polymer–colloid mixtures. We derive the scaling behavior with density, and find important deviations from the AO model and other ideal-polymer theories. We also calculate the depletion potential between spheres within our new "polymers as soft colloids" coarse-graining scheme,[38–41] where each polymer is represented by a single particle, interacting via a density-dependent effective potential. Here we again find good agreement with the direct MC results for the dilute regime, but for $\rho/\rho^* > 2$, significant deviations occur. In Sec. IV, we discuss the effect of polymer density on the virial coefficients between two colloids, and relate this to phase behavior of polymer–colloid mixtures.

II. DEPLETION POTENTIAL BETWEEN TWO WALLS

A. Surface tension near a single wall and the depletion potential at contact

Immersing a single hard wall (or plate) into a bath of nonadsorbing polymers in a good solvent reduces the number of configurations available to the polymers. This in turn results in an entropically induced depletion layer $\rho(z)$ near the wall, discussed in more detail, for example, in Paper I. Associated with the creation of this depletion layer is an interfacial free energy cost per unit area A, i.e., a wall–fluid surface tension $\gamma_w(\rho)$, which typically depends on the bulk density ρ, or equivalently the bulk chemical potential μ.[42] Bringing two such walls, of area A, together from an infinite distance apart to a distance x where the two depletion layers begin to overlap, changes the total free energy of the polymer solution. This change in the free energy or grand potential Ω per unit area is called the depletion potential $W(x) \equiv (\Omega(x) - \Omega(x = \infty))/A$.[42] When $x = 0$, i.e., when the two walls are brought into contact, the depletion potential reduces to the simple form

$$W(0) = -2\gamma_w(\rho), \tag{1}$$

reflecting the fact that the two depletion layers are completely destroyed.

In Paper I, we used an extension of the Gibbs adsorption equation to express the surface tension near a single wall as

$$\gamma_w(\rho) = -\int_0^\rho \left(\frac{\partial \Pi(\rho')}{\partial \rho'}\right)\hat{\Gamma}(\rho')d\rho'. \tag{2}$$

The derivation of this equation can be found, for example, in Refs. 25 and 43. Here $\Pi(\rho)$ is the osmotic pressure of the polymer solution, and $\hat{\Gamma}(\rho)$ is the reduced adsorption near a single wall, defined as

$$\hat{\Gamma}(\rho) = -\frac{1}{\rho}\frac{\partial(\Omega^{\text{ex}}/A)}{\partial\mu} = \int_0^\infty \left(\frac{\rho(z)}{\rho} - 1\right)dz, \tag{3}$$

where Ω^{ex}/A is the excess grand potential per unit area. In Paper I, we used computer simulations of a SAW polymer solution in a good solvent near a wall to calculate $\rho(z)$ and $\hat{\Gamma}(\rho)$ for several values of ρ/ρ^*. As discussed in Paper I, the SAW on a cubic lattice is a very good model for polymers in a good solvent. In the scaling limit, where the length L tends towards infinity, its properties are universal, and agree with experiments on polymers in the same good solvent regime.[33,36] For example, the radius of gyration scales as $R_g \sim L^\nu$, where ν is the Flory exponent, taken to be $\nu = 0.588$ in this paper. By using an accurate fitting form which takes into account the correct scaling behavior, we expressed $\hat{\Gamma}(\rho)$ for all densities in the dilute and semidilute regimes. When this was combined with a RG expression for the pressure, we were able to calculate the surface tension $\gamma_w(\rho)$ as a function of density through Eq. (2). Our results agreed very well with some recent RG calculations.[44]

Here we use $\gamma_w(\rho)$ together with Eq. (1) to directly calculate the depletion potential at contact, as shown in Fig. 1. These results are also compared to direct computer simulations of $L = 100$ SAW polymers.[38,39] Even though the L
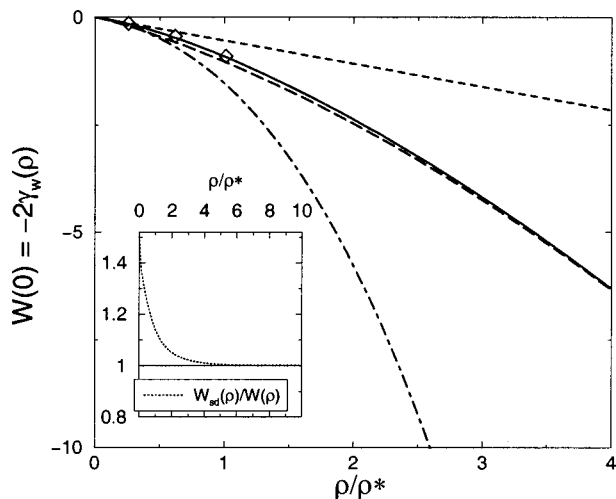
FIG. 1. Depletion potential between two walls or plates at contact $W(0)$ $=-2\gamma_w(\rho)$ per unit area R_g^2. The full line results from Eq. (2), while the long-dashed line comes from the simpler semidilute scaling expression (6). The diamonds denote previously published $L=100$ SAW simulation results (Ref. 39). The dashed line represents the simple ideal polymer form $W_{id}(0)$, given by Eq. (9), while the dot-dashed line shows the naive improvement obtained by substituting the true polymer osmotic pressure for the ideal polymer pressure. These two Asakura–Oosawa-type approximations bracket the correct result. The inset shows the strength of the simpler semidilute scaling expression relative to the the full potential at contact (dotted line). The two coincide for higher densities. In the low density limit, the semidilute scaling expression overestimates the true value at contact by a factor 1.5.

=100 simulations have not quite reached the scaling limit, the well depths at contact are remarkably well reproduced, a result also found by Tuinier and Lekkerkerker[25] with a similar theory.

B. A simple theory for the depletion potential

The simplest approximation for the depletion potential at finite separation x would be a linear form with a slope equal to the osmotic pressure. This follows because $\Pi(\rho)x$ is proportional to the work per unit area produced by the osmotic pressure,

$$W(x)=W(0)+\Pi(\rho)x; \quad x \leqslant D_w(\rho),$$

$$W(x)=0; \quad x > D_w(\rho), \tag{4}$$

where the range is given by

$$D_w(\rho)=-\frac{W(0)}{\Pi(\rho)}=\frac{2\gamma_w(\rho)}{\Pi(\rho)}. \tag{5}$$

We note that this approximation is similar to that adopted by Joanny, Leibler, and de Gennes who, in their pioneering paper,[18] approximated the force between two plates as constant for $x \leqslant \pi\xi(\rho)$ and zero for $x > \pi\xi(\rho)$, where $\xi(\rho)$ is the correlation length, the relevant length-scale in the semidilute regime.[33,36] This also results in a linear depletion potential.

In Fig. 2 we compare our simple linear potential to the direct SAW simulations. The overall agreement is striking. The only (small) deviation occurs at larger distances x where the true potential rounds off and develops a very small maximum before going to zero.[45] The range $D_w(\rho)$ of this simple
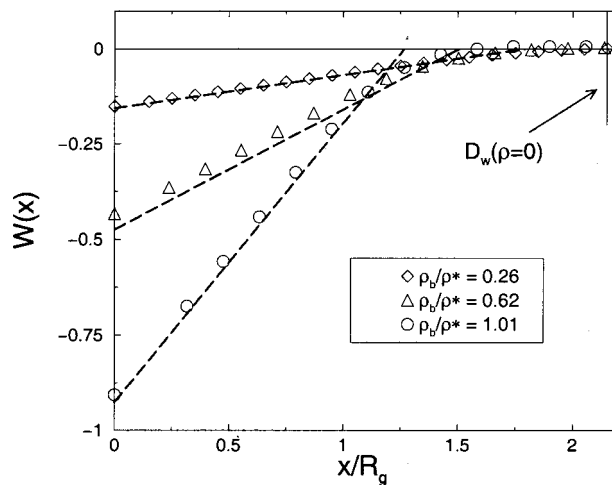

FIG. 2. Depletion potential between two walls or plates $W(x)$ per unit area R_g^2. The symbols denote simulations for $L=100$ SAW polymers, the straight lines are the simple theory of Eq. (4), which provides a near quantitative fit to the simulation data. The range $D_w(\rho=0)\approx2.15$ is shown as a vertical line. Note how much the range decreases with density, even for these results in the dilute regime.

potential decreases with ρ/ρ^*. In fact, as shown in Fig. 3, the largest relative rate of decrease occurs in the dilute regime, so that at $\rho/\rho^*=1$, the range is $D=1.25R_g$, about 58% of the low density limit of $D\approx2.15$. In general, the range of a potential is not always unambiguously defined.[46] Of course for our linear one it is, and this simple definition would seem a very reasonable definition for the range of the full depletion potentials depicted in Fig. 2.

C. Scaling theory for the depletion potential in the semidilute regime

Further simplifications occur in the semidilute regime. For example, when the scaling forms[33] for the osmotic pres-
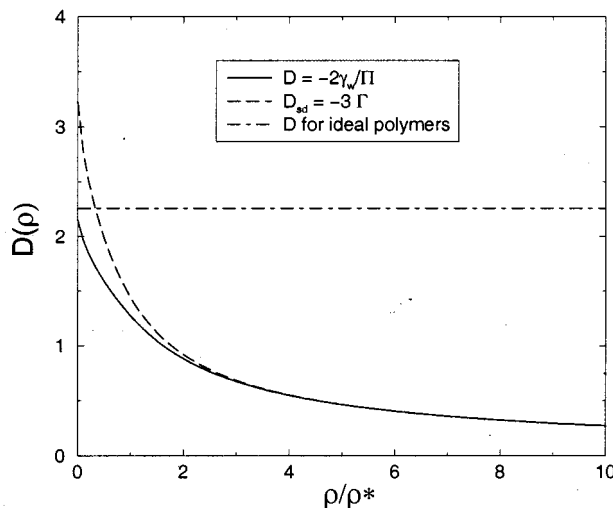

FIG. 3. Comparison of the range $D_w(\rho)$ of the depletion potential with the simpler semidilute scaling expressions $D_{sd}(\rho)$, both in units of R_g. As density increases well into the semidilute regime, the two expressions coincide. In the low density limit the semidilute expression is exactly 1.5 times the full expression. Note how much the range differs from the density independent result for noninteracting polymers $D_{id}=4/\sqrt{\pi}\approx2.26$.

sure, $\Pi \sim \rho^{3\nu/(3\nu-1)}$ and the reduced adsorption $\hat{\Gamma} \approx -\xi(\rho)$ $\sim \rho^{-\nu/(3\nu-1)}$ are used in Eq. (2), then, as shown in Paper I, the integral simplifies and the potential at contact takes on the very simple form,

$$W_{sd}(0)=3\Pi(\rho)\hat{\Gamma}(\rho) \sim \rho^{2\nu/3\nu-1} \approx \rho^{1.539}. \tag{6}$$

The linear depletion potential (4) then reduces to

$$W_{sd}(x)=\Pi(\rho)(3\hat{\Gamma}(\rho)+x); \quad x \lesssim D_{sd}$$
$$W_{sd}(x)=0; \quad h>D_{sd}, \tag{7}$$

and the range simplifies

$$D_{sd}(\rho)=-3\hat{\Gamma}(\rho) \sim \rho^{-\nu/(3\nu-1)} \approx \rho^{-0.770}. \tag{8}$$

As can be seen in Figs. 1 and 3, these simple expressions for the well-depth and the range work remarkably well in the semidilute regime, especially for $\rho/\rho^* > 2$.

Deviations do occur for low densities since according to Eqs. (1) and (2), $W(x=0) \approx 2\Pi(\rho)\hat{\Gamma}(\rho)$ for $\rho \to 0$, the same form as for ideal polymers. Equation (6) therefore overestimates the well depth by a factor 1.5, as can be seen in the inset of Fig. 1. In the same limit the range of the depletion potential reduces to the functional form $D=-2\hat{\Gamma}(\rho)$, so that Eq. (8) also overestimates the range at low densities by a factor 1.5, as can be seen in Fig. 3.

In the semidilute regime one can identify $\hat{\Gamma}(\rho) \approx -\xi(\rho)$.[33] Therefore the ansatz $D_w(\rho)=\pi\xi(\rho)$, originally postulated by Joanny *et al.*,[18] is very close to $D_{sd}(\rho)=-3\hat{\Gamma}$, the expression we derived for the range of the depletion potential in the semidilute regime. Their potential is therefore quite accurate in the semidilute regime, but overestimates the range and the well-depth by a factor slightly larger than 1.5 in the dilute limit.

D. Comparison with theories for noninteracting polymers between two walls

For completeness we compare the results obtained in the previous section to those for ideal polymers, first obtained by Asakura and Oosawa in 1954.[5] Their (exact) depletion potential can be quite accurately approximated by a simple linear form,[39]

$$W_{id}(x)=\rho\left(-\frac{4}{\sqrt{\pi}}+x\right); \quad x \leqslant \frac{4}{\sqrt{\pi}}R_g,$$
$$W_{id}(x)=0; \quad x>\frac{4}{\sqrt{\pi}}R_g. \tag{9}$$

However, for interacting polymers, this is only true in the limit $\rho \to 0$; the validity of this expression rapidly deteriorates with increasing density. As shown in Fig. 1, Eq. (9) underestimates the well depth for all but the lowest densities, while, as shown in Fig. 3, it overestimates the range at all densities. One might think that replacing the ideal pressure $\Pi(\rho)=\rho$ in Eq. (9) by the pressure of an interacting polymer system would bring an improvement for the well depth, even if this does not improve the approximation for the range. Instead, as shown in Fig. 1, this naive approach leads to a severe overestimate of the well-depth. In fact, for the semi-

dilute regime, the contact value of this naive ''improvement'' would scale as $W_{id}^{naive}(0)=(4/\sqrt{\pi})\Pi(\rho) \sim \rho^{3\nu/(3\nu-1)} \approx \rho^{2.309}$ instead of the correct $W(0) \sim \rho^{2\nu/(3\nu-1)} \approx \rho^{1.539}$ scaling. Even for $\rho/\rho^*=1$ the differences are significant: $W(0)=-0.93$, while $W_{id}(0)=-0.54$ and $W_{id}^{naive}(0)=-1.68$. For $\rho/\rho^*=10$, $W(0)=-25.4$, $W_{id}(0)=-5.4$, and $W_{id}^{naive}(0)=-208$! In other words, the simple heuristic ansatz is almost never a real improvement; for interacting polymers, the Asakura–Oosawa potential between two plates is only accurate at the very lowest densities.

III. DEPLETION INTERACTIONS BETWEEN SPHERES

We now turn to the polymer induced depletion interaction between two hard spheres. Similarly to the case of two walls, when the surfaces of two such spheres are brought to within a distance where their depletion layers begin to overlap, the total free energy of the system changes; this change again defines the depletion potential.

Since we found in Paper I that the surface tensions associated with the polymer depletion layers around a single sphere show behavior which differs from that of ideal polymers or that of the AO model, we expect to find qualitative differences in the depletion potentials as well. The trends are expected to be similar to those found for the depletion potential between two walls, namely that the range should decrease and the well depth should increase with increasing polymer concentration.

A. Full SAW polymer simulations

To calculate the polymer induced depletion potential between two spheres directly, we performed grand-canonical simulations of $L=500$ SAW polymers on a lattice of size $240 \times 150 \times 150$, and computed the osmotic pressure or force exerted on two hard spheres placed in the same simulation box. The configuration space of polymers was sampled in the grand canonical ensemble with a combination of configurational bias Monte Carlo and pivot moves.[4] The depletion force on the spheres was obtained from the ratio of the acceptance of virtual inward and outward moves of the spheres.

In Fig. 4 these forces are shown for three different size ratios $q=R_g/R_c$, namely, $q=0.67$, $q=1.05$, and $q=1.68$. For the first two size ratios, we computed the forces at three densities, $\rho/\rho^*=0.58$, $\rho/\rho^*=1.16$, and $\rho/\rho^*=2.32$.[42] For $q=1.68$, this was only done for the lower two densities. As expected, for a fixed size ratio, the range decreases, and the force at contact increases with increasing polymer density. For a given density, the range appears to contract slightly with increasing q, as might be expected, since the polymers can deform more readily around the smaller colloids (see the Appendix for further discussion of this point). In each simulation we keep the size of the polymers fixed, so that the larger size ratios essentially correspond to smaller spheres. The computational cost scales with the size of the simulation box, which roughly sets the number of polymers needed to achieve a density ρ/ρ^* in the accessible volume left by the colloids.

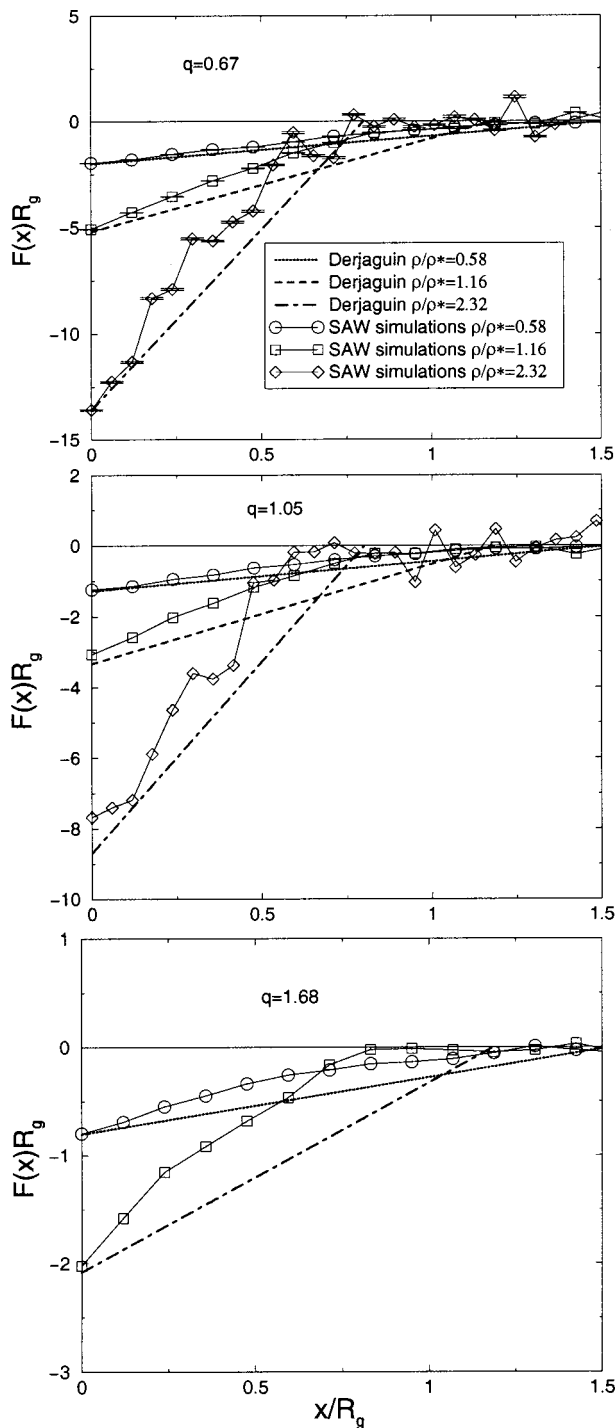The force can then be integrated to obtain the effective depletion potential,

FIG. 4. Depletion forces between two spheres for three size ratios q, as a function of x, the distance between the surface of the two spheres. The symbols denote $L=500$ SAW computer simulations for three densities: $\rho/\rho^*=0.58$ (circles), $\rho/\rho^*=1.16$ (squares), $\rho/\rho^*=2.32$ (diamonds), the solid lines are to guide the eye. These are compared to results from the Derjaguin approximation for the same size ratios and densities: $\rho/\rho^*=0.58$ (dotted lines), $\rho/\rho^*=1.16$ (dashed lines), and $\rho/\rho^*=2.32$ (dot-dashed lines).

$$V(x) = -\int_x^\infty F(y)dy. \qquad (10)$$

Results are shown in Fig. 5 for the same parameters as in Fig. 4. Because the curves are integrated, they appear
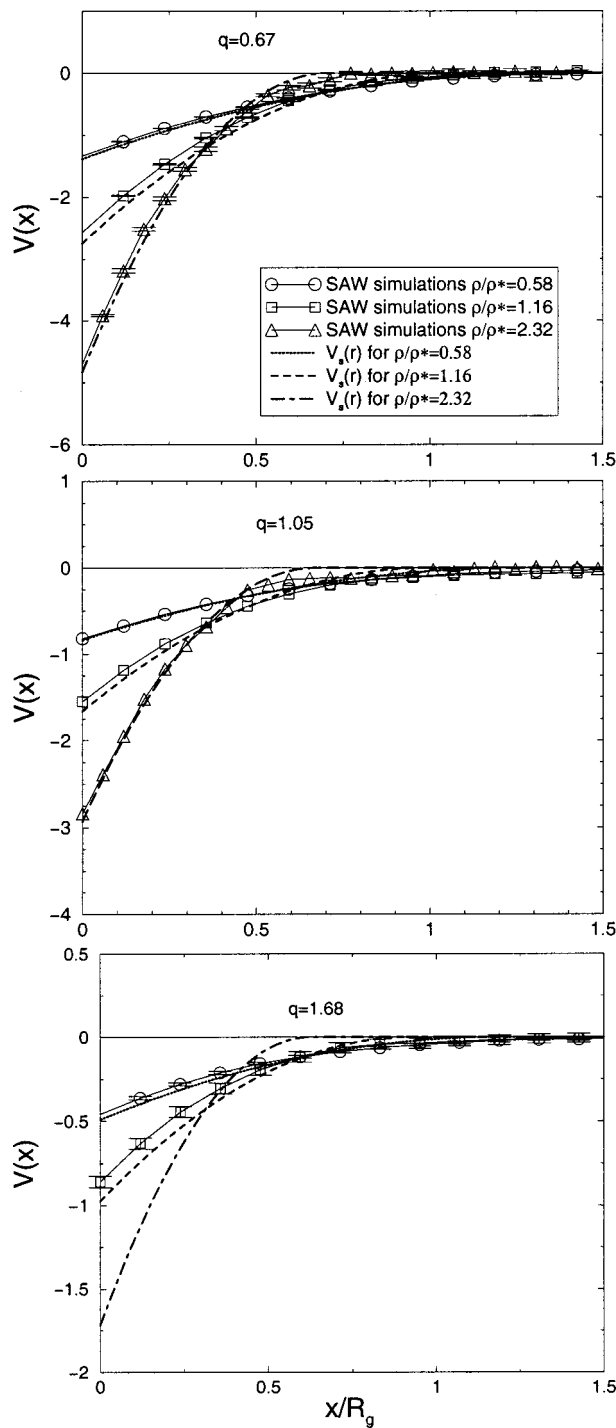
FIG. 5. Depletion potentials between two spheres for the same set of parameters as in Fig. 4. These are compared to the semiempirical depletion potential $V_s(r)$ [Eq. (17)] for the same size ratios and densities.

smoother than the forces. There may still be some residual error in the potentials, which might explain why the range for the highest density seems slightly larger for the potential than for the force. Also, the errors are too large to determine whether or not there is a repulsive bump in the potential. If it does exist, it is probably very small.[47] This is in contrast to hard-core systems, where such bumps can be pronounced.[20,48,49] The weakness or absence of a repulsive barrier in the case of interacting polymers can probably be

traced to the very low monomer concentration c. For shorter polymers, whose behavior deviates significantly from the $L \to \infty$ scaling limit, and where a substantial monomer density c can more easily be achieved, such repulsive bumps might occur more readily.[50]

As expected, the range decreases while the force at contact and the potential well-depth increase with increasing polymer density. For a fixed density and polymer size R_g, the force at contact and the well-depth decrease as the spheres become smaller (or q becomes larger). The same effect occurs for ideal polymers,[30] where it has a simple geometric origin: the volume of a depletion layer of a given width $\sim R_g$ decreases with decreasing size of the hard spheres.

B. The Derjaguin approximation for interacting polymers

In the case of two walls, the well-depth at contact has a clear interpretation in terms of the complete destruction of two depletion layers, and can therefore be expressed as a simple function of the wall–polymer surface tension $\gamma_w(\rho)$, as shown in Eq. (1). For two spheres, the depletion layers do not completely overlap, and the depletion potential at contact is related to the surface tension of polymers surrounding two spheres in a dumbbell type configuration. A simple expression for the well depth at contact in terms of the surface tension $\gamma_s(\rho)$ is therefore less obvious.

One way to make contact with the two wall case is to use the Derjaguin approximation,[37] which relates the force between two spheres of radius R_c to the potential between two walls, $W(x)$, in the following way:

$$F^{\text{Derj}}(x) = \pi R_c W(x), \tag{11}$$

where x is the distance between the surfaces of the two spheres. In principle this approximation should only be accurate for very small size ratios q, i.e., for very large colloids. However, as shown in the Appendix, we expect there to be a cancellation of errors, related to the deformation of the polymers around spherical particles, which makes the Derjaguin approximation work much better than one would naively expect. This is confirmed in Fig. 4, where the Derjaguin expression for the force, taken from Eq. (4) and Eq. (11), is shown to be a surprisingly good approximation. It is most accurate for the smallest q, as expected, but even for $q = 1.68$, where normally one would not expect the Derjaguin approximation to be useful at all, it is still reasonable.

By combining Eq. (4) with Eqs. (10) and (11) we obtain the following Derjaguin expression for the depletion potential between two spheres:

$$V^{\text{Derj}}(x) = -\frac{\pi}{2} R_c \Pi(\rho)(D_w(\rho) - x)^2 \tag{12}$$

for $0 \leq x \leq D_w(\rho)$; $V^{\text{Derj}}(x) = 0$ for $x > D_w(\rho)$. By the nature of the Derjaguin approximation, $D_w(\rho)$ is the same range as found for two walls in Eq. (5). This simple potential is compared in Fig. 6 to the direct $L = 500$ SAW simulation results for $q = 1.05$. The correspondence is surprisingly good given the large size ratio q, although it is not quantitative as in the wall–wall case. Similar results are found for the two other
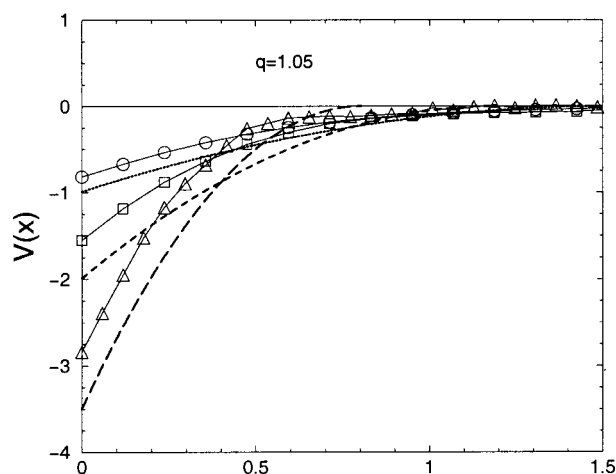
FIG. 6. Comparison of the $L = 500$ SAW computer simulations for the depletion potential with the Derjaguin approximation of Eq. (12) for $q = 1.05$. The symbols are the same as in Fig. 4.

size ratios. Overall, the Derjaguin approximation overestimates the well-depth, a consequence of the slightly longer ranged forces found in Fig. 4. Again, the cancellation of errors found for the simpler AO model in the Appendix helps explain why Eq. (12) works reasonably well in a regime where the Derjaguin approximation would normally break down.

C. The Derjaguin approximation in the semidilute regime

We now turn to the scaling behavior of the depletion potential in the semidilute regime. By using the simple expression for the range $D_{sd}(\rho)$ given in Eq. (8), the Derjaguin approximation for the depletion potential (12) reduces to

$$V_{sd}^{\text{Derj}}(x) = -\frac{\pi}{2} R_c \Pi(\rho)[3\hat{\Gamma}(\rho) + x]^2 \tag{13}$$

for $x \leq D_{sd}(\rho)$; $V_{sd}^{\text{Derj}}(x) = 0$ for $x > D_{sd}(\rho)$. For two walls, the simplified expression (8) for the range overestimates the true range by a factor 1.5 in the low-density limit. Here the overestimate is slightly larger, since, as shown in the Appendix, the deformation of the polymers around a single colloid reduces the depletion layer width for decreasing sphere size R_c. Similarly the well-depth at contact is also overestimated in the low density limit, but now by a factor $\lim_{\rho \to 0} V_{sd}^{\text{Derj}}(0)/V^{\text{Derj}}(0) = 2.25$. In the semidilute regime the two expressions come closer for increasing density. For example, at $\rho/\rho^* = 2$ the overestimate at contact is only $V_{sd}^{\text{Derj}}(0)/V^{\text{Derj}}(0) = 1.09$, while for $\rho/\rho^* = 4$ the two expressions are within 1% of each other. If in addition we assume that $\hat{\Gamma}(\rho) \approx -\xi(\rho)$ then the expression in Eq. (13) is again very similar to the form proposed by Joanny *et al.*[18] for two spheres (3 being replaced by π). Our arguments therefore provide an a-posteori justification of the validity of their potential for the semidilute regime. In the dilute regime it will overestimate the attraction in the same way as Eq. (13) does.

Given that we now have a reasonably accurate depletion potential between two spheres, namely, Eq. (12), it seems
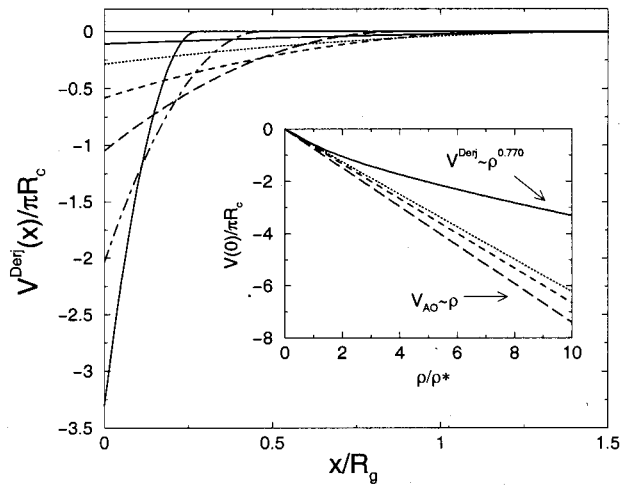
J. Chem. Phys., Vol. 117, No. 4, 22 July 2002

Polymer induced depletion potentials   1899

FIG. 7. Scaled depletion potential $V^{\mathrm{Derj}}(x)/(\pi R_c)$ for interacting polymers. From top to bottom the densities are $\rho/\rho^* = 0.2$, 0.5, 1, 2, 5, and 10, respectively. In the semidilute regime the well-depth increases like $\rho^{0.770}$ while the range decreases as $\rho^{-0.770}$. Inset: Scaled well depth at contact $V^{\mathrm{Derj}}(0)/(\pi R_c)$ for interacting polymers (solid line), compared to the scaled well depth $V_{\mathrm{AO}}(0)/(\pi R_c)$ for the AO potential of Eq. (A1) with $R_{\mathrm{AO}} = R_{\mathrm{AO}}^{\mathrm{eff}}$ given by Eq. (A3). The scaled AO potentials are shown for $R_c = 10R_g$, (dotted line), $R_c = 2R_g$ (dashed line), and $R_c = 0.5R_g$ (long-dashed line). In contrast to the Derjaguin approximation expressions, the AO potential does not satisfy perfect scaling with R_c. The well-depth scales linearly with ρ. The range is $2R_{\mathrm{AO}}^{\mathrm{eff}}$, and is independent of ρ.
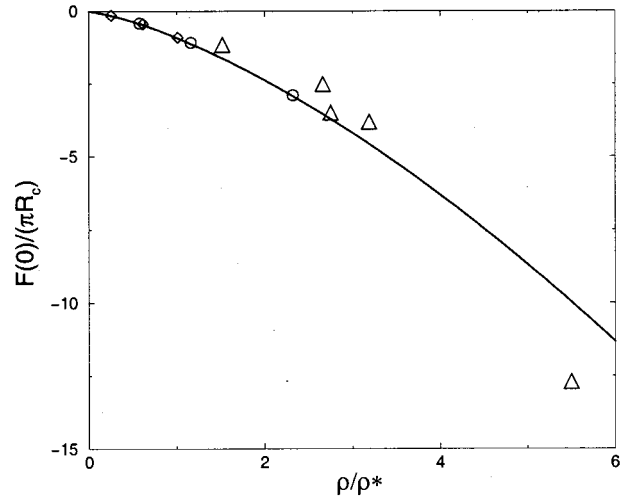

FIG. 8. Comparison of the force at contact with the Derjaguin expression, Eq. (11). The circles are taken from the SAW simulations depicted in Fig. 4. On the scale of this graph, the three size ratios lead to virtually identical results at each density. The triangles denote $F(0)/(\pi R_c)$ from the fluctuation bond model simulations of Yethiraj and Dickman (Ref. 22). The diamonds are from previous $L = 100$ SAW simulations of $W(0)$, the interaction between two plates (Refs. 38, 39). The curve denotes $W(0) = -2\gamma_w(\rho)$, the expected result for the Derjaguin approximation.

fruitful to examine how this expression varies with density. We do this in Fig. 7 for a number of densities in the dilute and the semidilute regimes. Since within the Derjaguin approximation the depletion potential (12) always scales with R_c, the curves in the plot can be used for all size ratios. Of course one should keep in mind that the Derjaguin approximation becomes progressively less accurate for decreasing R_c/R_g. With this caveat in mind, the well-depth at contact for polymers in a good solvent scales as

$$V_{\mathrm{sd}}^{\mathrm{Derj}}(0) \sim \rho^{\nu/(3\nu-1)} \approx \rho^{0.770} \tag{14}$$

in the semidilute regime. This is exactly half the exponent with which the well-depth at contact scales for two walls in the semidilute regime [see Eq. (6)], which can be understood as follows: Within the Derjaguin approximation the force scales as $F(0) = \pi R_c W(0) \sim \rho^{2\nu/(3\nu-1)}$; the potential is then obtained through Eq. (10) by integrating this force over a range $D(\rho) \sim \rho^{-\nu/(3\nu-1)}$. These two effects result in the scaling seen in Eq. (14). On the other hand, by nature of the Derjaguin approximation, the range is the same as that shown in Fig. 3 for the wall–wall case, i.e., it decreases line $D_w(\rho) \sim \rho^{-0.770}$.

An expression similar to Eq. (13) has been derived by Fleer, Scheutjens, and Vincent (FSV).[19] They replace R_{AO} in the full AO potential (A1) by $2\hat{\Gamma}(\rho)$, and the density ρ by $\Pi(\rho)$. In its original applications,[51] the FSV theory was used with a self-consistent field theory to calculate $\hat{\Gamma}(\rho)$, and a simple Flory Huggins prescription for $\Pi(\rho)$. This leads to $\hat{\Gamma}(\rho) \sim \rho^{-(1/2)}$ scaling behavior which is more appropriate for polymers near the theta point.[33] However, one could easily generalize the FSV approach and include the $\hat{\Gamma}(\rho)$ and

$\Pi(\rho)$ appropriate for polymers in a good solvent. For the semidilute regime the FSV approach would then lead to an underestimate of the range by a factor 2/3, while for small q, where the Derjaguin approximation is quite accurate, it would underestimate the attraction at contact by a factor of about 4/9. On the other hand, in the dilute regime, this approach should perform better, although for increasing q it is expected to overestimate the attraction at contact in a very similar way to the effects seen for the AO model in Fig. 15(a). This is because the FSV model ignores the deformation of polymers near a spherical surface. It would be better to use the $D(\rho)$ appropriate for a spherical particle; this results in a potential similar in spirit to an interesting recent proposal by Tuinier and Lekkerkerker.[52]

D. An accurate semiempirical depletion potential

As can be seen in Fig. 4, the Derjaguin approximation seems to be particularly accurate for the force at contact. In fact, when we plot $F(0)/(\pi R_c)$ versus ρ/ρ^* in Fig. 8, the results for the three size ratios are very close to each other at each of the densities studied, and their value is well described by $W(0) = -2\gamma_w(\rho)$, as expected for the Derjaguin approximation [see Eq. (11)]. Furthermore, we analyzed the computer simulation data of Dickman and Yethiraj,[22,53] which used the fluctuation bond model (FBM) for size ratios ranging from $q = 1.3$ to $q = 3.5$, and find similar agreement in Fig. 8. Keep in mind that the FBM results are for shorter chains ($L = 20-100$), and that the error bars appear to be larger than those in our simulations. Since for $q = 3.5$ the Derjaguin approximation (11) should not be valid at all, this does suggest that the expression,

$$F(0) = \pi R_c W(0) = -2\pi R_c \gamma_w(\rho), \qquad (15)$$

may hold because of an (approximate) sum rule, and that the agreement is not fortuitous.

The surprising accuracy of expression (15) for the force at contact can be exploited to derive a more accurate effective potential than that found by the direct application of the Derjaguin approximation. We assume the same linear force between two spheres as found in the previous two sections, but now with a modified range,

$$D_s(\rho) = D_w(\rho) \frac{R_{AO}^{eff}(R_c)}{R_g}, \qquad (16)$$

where the effective shrinking of the range due to the deformation of the polymers around the HS has been taken into account via Eq. (A3). Although this deformation effect is calculated for ideal polymers, we expect it to be a good first approximation for the *relative* deformation of interacting polymers around a sphere. The resulting simple linear expression for the force can now be integrated up via Eq. (10) to give the depletion potential,

$$V_s(x) = \frac{\pi}{2} R_c W(0) D_s(\rho) \left(1 - \frac{x}{D_s(\rho)} \right)^2 \qquad (17)$$

for $x \leq D_s(\rho)$. $V_s(x) = 0$ for $x > D_s(\rho)$. Our new semiempirical potential works remarkably well, as can be seen in Fig. 5 for the three size ratios. Even for $q = 1.68$, corresponding to the smallest colloids, this potential is significantly better than the Derjaguin expression (12), suggesting that Eq. (17) can be considered a nearly quantitative representation of the depletion potential induced between two spheres by SAW polymers for a surprisingly wide range of q's. Since the semiempirical potential (17) reduces to the regular Derjaguin form (12), if $D_s(\rho)$ is replaced by $D_w(\rho)$, its scaling properties with density are the same as those discussed in the previous subsections.

E. Comparison with theories for noninteracting polymers

It is interesting to compare the results for interacting polymers with the results for noninteracting polymers. First, just as was found for two walls, the range for the depletion potential is independent of density for noninteracting polymers. This is true both for the simpler AO model,[6] as well as for more sophisticated theories and computer simulations.[30,54,55] For a given R_g, using a theory based on noninteracting polymers will always overestimate the range compared to the interacting case. Since for our accurate semiempirical potential the range $D_s(\rho)$ is related to $D_w(\rho)$ by a density independent factor related to q, the *relative* overestimate in the range for the spherical case should be close to that found when comparing a noninteracting theory to an interacting one for the range of the depletion potential between two plates, as done in Fig. 3.

For the case of two walls the absolute value of the well-depth at contact given by ideal polymers or the AO model was *underestimated* with respect to the interacting case. Within the Derjaguin picture of Eq. (11), this implies that noninteracting polymer models will underestimate the force

at contact $F(0)$ for two spheres in a bath of interacting polymers by a similar factor to that shown for $W(0)$ in Fig. 1.

In the inset of Fig. 7 we compare the scaled well-depth at contact $V^{Derj}(0)/(\pi R_c)$ for the Derjaguin approximation with that of the AO model, given in Eq. (A1), where an effective range parameter R_{AO}^{eff}, given by Eq. (A3) in the Appendix, was used to take into account the deformation of the polymers around the colloids. For a given R_c, the well-depth $V_{AO}(0)$ scales linearly with ρ, which is now an *overestimate* compared to the result for interacting polymers. The origin of this behavior can be easily understood; while the strength of the force is strongly underestimated by the AO model, the range is overestimated. Therefore the integral in Eq. (10) shows a compensation of errors. This explains why, at low densities, the AO approximation well depth is very close to the interacting polymer result. For example for $q = 0.1$ we find for $\rho/\rho^* = 1$ that $V_s(0)/V_{AO}(0) \approx 0.93$ while for $\rho/\rho^* = 10$ this ratio is still only 0.56. Attempting a naive improvement by replacing ρ in the AO expression by the true pressure of a polymer solution results in a worse approximation for all densities.

F. Polymers as soft colloids

When modeling polymer–colloid mixtures, the colloids are usually treated as single particles. It thus seems natural to attempt the same for the polymers. We have recently succeeded in modeling linear polymers as "soft colloids,"[38–41,56] where each polymer is replaced by a single particle centered on its CM. Different coils interact via an effective pair potential acting between their CM. These effective interactions $v(r;\rho)$ between the CM of the polymers are extracted from the radial distribution functions $g(r)$ with an Ornstein–Zernike inversion technique. This procedure is justified by a theorem which states that for any given $g(r)$ and ρ there exists a unique pair-potential which reproduces that radial distribution function.[57,58] Our $v(r;\rho)$ have a near Gaussian shape, with an amplitude of order $2k_BT$ and a range of the order of the radius of gyration R_g. For $\rho/\rho^* \leq 2$ accurate analytic forms as a function of r/R_g and ρ/ρ^* are available.[41]

Our input $g(r)$'s were generated by computer simulations of $L = 500$ SAW polymers on a cubic lattice, and so the density dependent effective potentials we derived will by definition reproduce the same CM pair structure as found in the underlying SAW polymer system. When used in conjunction with the compressibility equation,[3] these potentials also provide a very good representation of the equation of state.[39,41]

A similar coarse-graining procedure was followed to describe polymers near a flat wall,[38,39] where even ideal polymers form a depletion layer. If these were to be modeled as single particles, there would be no polymer–polymer interaction, but there would still be an effective polymer-wall interaction $\phi(z)$. We used direct simulations of $L = 500$ SAW polymers to extract the density profile $\rho(z)$ near a hard wall. The $\phi(z)$'s which reproduce the density profile at each given bulk density ρ were calculated using a wall-Ornstein–

Zernike procedure.[38,39] Again accurate analytic fits for densities $\rho/\rho^* \lesssim 2$ are available.[41]

Since our effective polymer–polymer potentials provide a very accurate representation of the pressure $\Pi(\rho)$, while the polymer–wall interactions are constrained to reproduce the correct density profile $\rho(z)$, and therefore the correct adsorption $\hat{\Gamma}(\rho)$, Eq. (2) implies that our soft-colloid approach will reproduce the correct wall–fluid surface tension $\gamma_w(\rho)$. This explains why our soft-colloid approach reproduces the correct value for $W(0)$,[38,39] the depletion potential at contact between two walls, since Eq. (1) implies that this can be expressed completely in terms of $\gamma_w(\rho)$. Similarly the slope of the potential is given by the osmotic pressure $\Pi(\rho)$ which is also accurately represented in the soft-colloid approach. Deviations with respect to direct simulations were only observed for larger distances z, where the soft-colloid approach produced a more pronounced repulsive bump in the depletion potentials.[38,39]

To calculate the depletion potential between spheres, we need to first derive the effective sphere-polymer CM potential $\phi(r)$ which would exactly reproduce the density profile $\rho(r)$ around a single sphere of radius R_c. This can again be done using an Ornstein–Zernike (OZ) technique to invert the density profiles.[41] These density profiles were calculated in Paper I, where we found that the range of the profiles shrinks with increasing density. The CM profiles can penetrate into the spheres because the polymers can deform around them, an effect which becomes more pronounced with decreasing sphere size (this does not happen in the monomer representation of course). Similarly, the effective potentials $\phi(r)$, derived with our inverse OZ approach, become relatively softer with decreasing R_c, as shown in Fig. 9.[41] For a fixed q the potentials become more repulsive for increasing density, just as was found for the polymer–wall case.[39] Note that this behavior is the opposite to that of the density profiles. Again, because these potentials are constrained to give the correct density profiles and related adsorptions, this soft colloid picture should also correctly reproduce the surface tension $\gamma_s(\rho)$ for a single sphere immersed in a bath of interacting polymers. The same should hold for the related one-body insertion free energies $F_1^{int}(\rho)$ described in Paper I.

1. Direct simulations of depletion potentials for polymers as soft colloids

The simulation of the depletion potentials induced by the "soft colloids" proceeds in a similar manner to the simulations with SAW polymers, described in Sec. III A. However, the implementation is much simpler, because the interactions are smooth and both types of particles are in continuous space. The simulations are also about two orders of magnitude faster, since each polymer is represented by only one particle, instead of the 500 units per polymer used for the SAW model. These simulations are compared for $q = 1.05$ in Fig. 10 to the direct SAW simulations. The agreement is very good for $\rho/\rho^* = 0.58$ and reasonable for $\rho/\rho^* = 1.16$. However for the highest density, $\rho/\rho^* = 2.32$, the soft-colloid approach breaks down. Exactly the same trend was found for the other two size ratios (not shown here). Since the soft-colloid approach reproduces the correct one-body densities
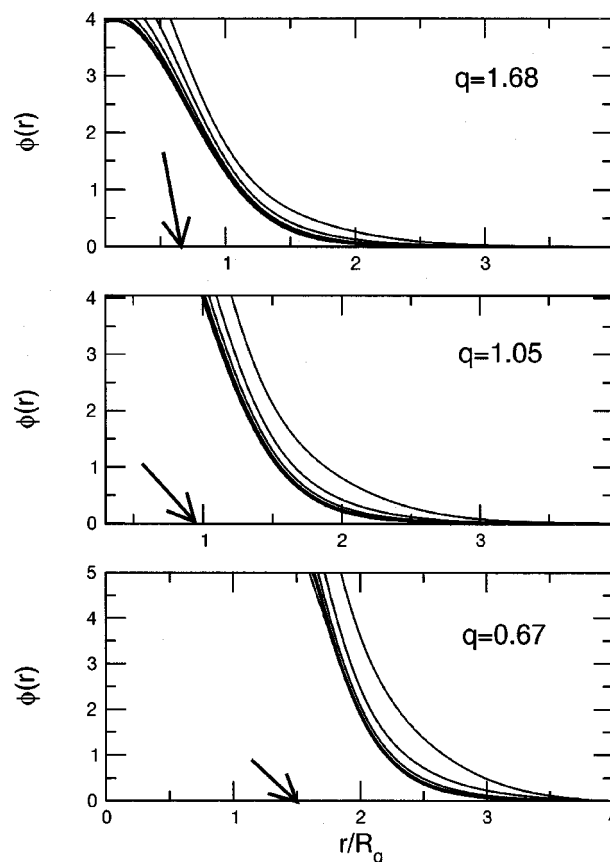

FIG. 9. The effective sphere–polymer potential $\phi(r)$ as a function of r, the distance to the center of the sphere for increasing polymer concentration (from left to right). These $\phi(r)$ are derived via an Ornstein–Zernike inversion technique such that they reproduce the CM density profiles around each sphere (Ref. 41). The arrows indicate the hard core radius of the spheres.

$\rho(r)$, and the correct one-body free energy $F_1^{int}(\rho)$ of immersing a single sphere into a bath of polymers for all densities ρ/ρ^* in the dilute and semidilute regimes, it is perhaps surprising that for the case of two spheres, it breaks down rather abruptly for higher densities. To further investigate this issue, we plot the polymer CM density profiles for two spheres fixed at distance $r = 2.6R_g$ for $q = 1.05$ and $\rho/\rho^* = 2.32$ in Fig. 11. This corresponds to a distance where the SAW $V(r)$ has effectively gone to zero. At this short distance the SAW polymers clearly penetrate more easily in between the two colloids than the soft particles do, resulting in less attraction between the colloids. A similar effect was found for polymers between two walls,[39] but there the fact that sum-rules constrain the value of the potential at contact means that this difference manifested itself instead in an enhanced repulsive bump in the potential. In both cases, we attribute the error in the soft-colloid approach under strong confinement and higher densities to a breakdown in the "potential superposition approximation,"[39] i.e., the assumption that a polymer confined between two surfaces feels an interaction which is simply the sum of the two interactions $\phi(r)$ with each separate surface. While this would be correct for simple fluids, it is not correct here, since the close presence of one wall affects the interaction of the polymers with the
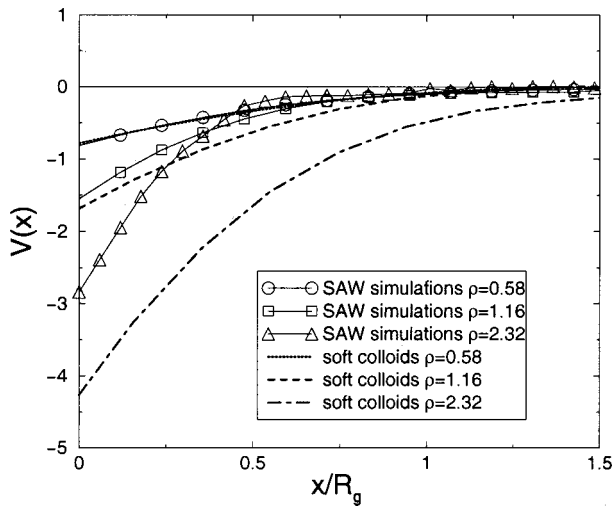
FIG. 10. Comparison of the direct SAW simulations of the depletion potential for $q = 1.05$ to direct simulations within the polymers as soft colloids approach.

second wall. This is essentially due to the deformability of the polymers, which is not correctly taken into account for strong confinement.

When we do a similar analysis of the densities as done in Fig. 11 for $\rho/\rho^* = 1.16$ however, the differences in the density profiles are very small, suggesting that the soft-particle picture is not yet breaking down. Coarse-graining polymers as soft colloids is expected to be most useful for $q \lesssim 1$, since once the polymers become much larger than the colloids, they can wrap around the colloids, an effect not easily treated in our coarse-graining scheme. Since for $q \lesssim 1$, we have found that phase-separation in polymer-colloid mixture sets in below $\rho/\rho^* \approx 1$,[72] the limit of physical stability is reached before we encounter problems with our coarse-graining scheme for polymer–colloid mixtures.
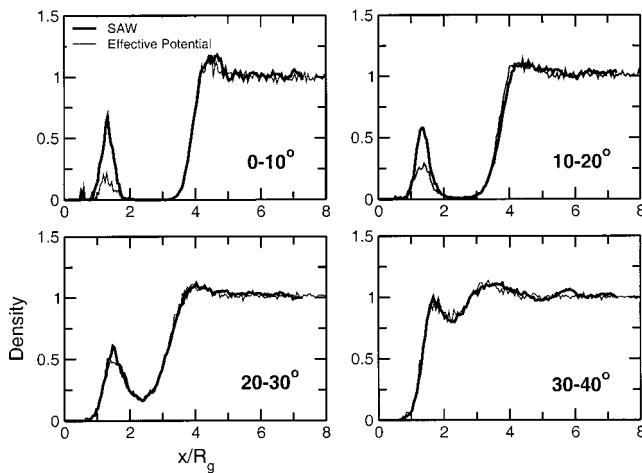

FIG. 11. Comparison of the direct $L = 500$ SAW simulations of the polymer CM density profile to direct simulations within the polymers as soft colloids approach for $q = 1.05$ and $\rho/\rho^* = 2.32$. One sphere is at 0, and the other is at $r = 2.6R_g$. The four graphs show the normalized density at a distance r, averaged over $(0–10°)$, $(10–20°)$, $(20–30°)$, and $(30–40°)$ with respect to the particle at the origin. The SAW polymers penetrate more easily between the colloids than the effective soft-colloids do.

2. Depletion potentials from the superposition approximation

To understand further the nature of the depletion potentials between the colloidal particles, mediated by the polymers in the "soft colloid" picture, we now turn to the superposition approximation, which expresses the two body depletion interactions in terms of one-body properties of a single colloid in a bath of soft polymers.

If one colloidal particle is fixed at the origin, and one is fixed at $\mathbf{r}$, then one can define an inhomogeneous one-particle density of the soft colloids $\rho^{(1)}(\mathbf{r}';\mathbf{0},\mathbf{r})$ for that fixed configuration of the two colloidal particles. The effective force induced between two colloidal HS by the soft colloids can then be written as[59,60]

$$\mathbf{F}(\mathbf{r}) = -\int \rho^{(1)}(\mathbf{r}';\mathbf{0},\mathbf{r}) \frac{\partial}{\partial \mathbf{r}'} \phi(r') d\mathbf{r}', \qquad (18)$$

where $\phi(r)$ is the interaction between the HS particles and the soft colloids. This expression has an obvious intuitive interpretation. The total force on a HS particle at $\mathbf{0}$ is the average of the sum of its interactions with all the soft colloids. If there are no other HS particles, then the equilibrium distribution will be spherically symmetric, and this force will be zero. However, if there is another HS particle at $\mathbf{r}$, it will perturb the density distribution of the soft colloids, which will in turn result in a different total force acting on the particle at $\mathbf{0}$. By definition, this is the effective or depletion force $\mathbf{F}(\mathbf{r})$ acting on a particle at $\mathbf{0}$, induced by the presence of a particle at $\mathbf{r}$.

Equation (18) is in principle exact, but requires knowledge of the soft colloid density around two colloidal HS. By approximating the full (cylindrically symmetric) one-body density $\rho^{(1)}(\mathbf{r}';\mathbf{0},\mathbf{r})$ by a superposition of the one-body density $\rho(r)$ around an isolated single sphere,[59]

$$\rho^{(1)}(\mathbf{r}';\mathbf{0},\mathbf{r}) = \rho(r')\rho(|\mathbf{r}-\mathbf{r}'|)/\rho, \qquad (19)$$

the effective depletion force (18) can be entirely expressed in terms of the (radially symmetric) problem of a single colloidal sphere immersed in a polymer solution. The results of such a calculation for $V(r)$ are compared in Fig. 12 for $q = 1.05$. For all three densities, the superposition approximation closely follows the direct simulations for the soft colloids. This implies that the full one-body density $\rho^{(1)}(\mathbf{r}';\mathbf{0},\mathbf{r})$ does not differ much from the simple superposition of Eq. (19), even for the highest density considered, $\rho/\rho^* = 2.32$. The reason for this is most likely that the effective polymer–polymer CM interaction $v(r)$ is rather weak. In a recent study, a similar good performance of the superposition approximation was found for a low density hard-core depletant when the HS-depletant interaction was fairly long ranged.[49] Good agreement was also found in a similar study of star-polymer colloid mixtures,[61] where accurate star-polymer–wall potentials[62] are derived based on a coarse graining approach.[63] In contrast, if the density of a hard-core depletant increases, then the superposition approximation is known to break down for increasing packing fraction.[60,64]

The fact that the superposition approximation works well for the soft colloids at the higher densities also raises an interesting question as to why the soft-colloid picture itself
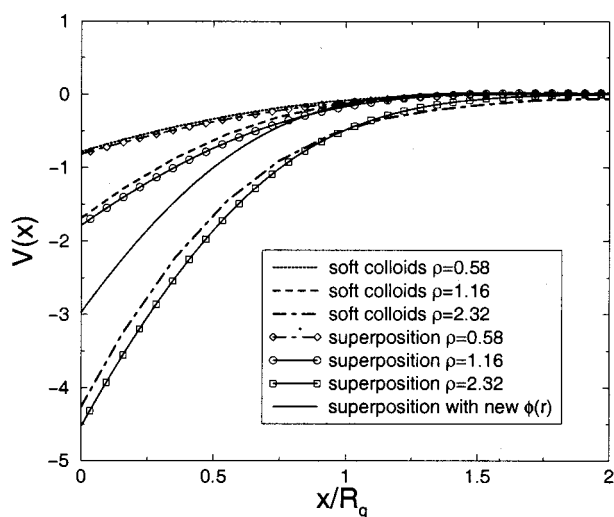
FIG. 12. Comparison of simulations of the depletion potential for $q=1.05$ within the soft-colloid approach with the superposition approximation of Eqs. (18) and (19). The thin solid line denotes the superposition calculation with $\rho(r)$ from $\rho/\rho^*=2.32$, but the potential $\phi(r)$ from the $\rho/\rho^*=1.16$ calculation. This illustrates the sensitivity of the depletion potentials to colloid–polymer CM interaction $\phi(r)$.
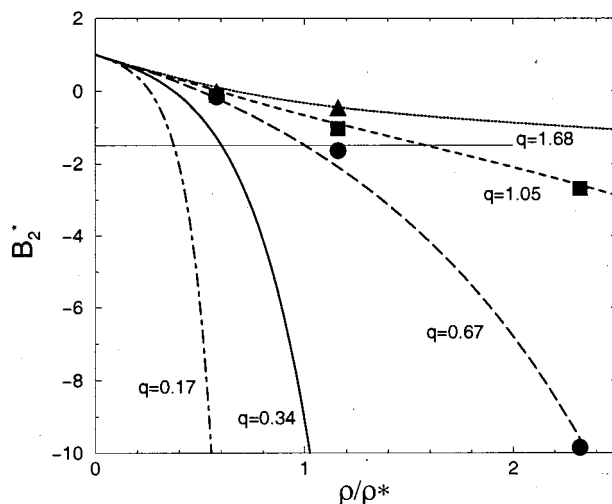

FIG. 13. Reduced virial coefficients as a function of polymer density: The symbols represent results from the computer simulations of $L=500$ SAW polymers for $q=0.67$ (circles), $q=1.05$ (squares), and $q=1.68$ (triangles). The straight lines are from Eq. (21). The good agreement shows that Eq. (17) provides a good representation of the depletion potential.

breaks down at the higher densities. By construction, the one-body density profiles are identical for the full polymer case and the soft-colloid picture. Presumably the reason for the difference in the two-body depletion interactions can be traced either to a large deviation from superposition for the full polymer case, or else to a breakdown of the potential superposition approximation, as discussed in Ref. 39. The influence of changing $\phi(r)$ is illustrated in Fig. 12, where we used the $\phi(r)$ appropriate for $\rho/\rho^*=1.16$ to calculate the depletion potential with the density profiles for $\rho/\rho^* =2.32$. This $\phi(r)$ is less repulsive than the true $\phi(r)$, and leads to a significant difference in the depletion potential. These depletion interactions are therefore quite sensitive to the exact form of $\phi(r)$.

In conclusion then, the superposition approximation works remarkably well for $\rho/\rho^*\lesssim 1$, the regime where the soft-colloid picture provides the most accurate representation of the true depletion potentials. Since the density profiles $\rho(r)$ can be easily calculated by our wall-OZ approach, this means that one only needs the polymer–colloid interaction $\phi(r)$ and the polymer–polymer interaction $v(r)$ as input to reliably calculate the full two-body depletion interactions from the superposition approximation.

IV. SECOND VIRIAL COEFFICIENTS AND PHASE DIAGRAMS

A useful measure of the strength of an interaction is the second osmotic virial coefficient B_2, since this is experimentally accessible through a measurement of the osmotic pressure at low densities.[65,66] Such virial coefficients are very sensitive to the strength and range of the depletion interaction.[28] A recent study[67] has shown that for many simple systems consisting of a HS like repulsion with an additional attractive potential, the location of the liquid–gas

or fluid–fluid critical point can be correlated with the point where the reduced virial coefficient $B_2^*=B_2/B_2^{HS}\approx -1.5$; here $B_2^{HS}=16\pi R_c^3/3$ is the virial coefficient of a HS system with radius R_c. For our depletion systems, the reduced virial coefficient is given by

$$B_2^*=1-\frac{3}{4R_c^3}\int_{R_c}^{\infty}x^2(\exp[-V(x)]-1)dx. \tag{20}$$

The direct simulation results depicted in Fig. 5 can be used to calculate B_2^*, and the results are shown in Fig. 13 for $\rho/\rho^*=0.58$, $\rho/\rho^*=1.16$, and for $\rho/\rho^*=2.32$. As expected, for a given density ρ/ρ^*, the B_2^* become progressively more negative with decreasing q. Although we don't include any explicit error bars in our plots, these may be rather large for increasing attraction because they appear exponentially in Eq. (20).

We found in the previous sections that a simple semi-empirical potential $V_s(x)$, given by Eq. (17), provides a nearly quantitative description of the depletion potentials between two spheres. It turns out that for this potential the virial coefficient can be integrated analytically,

$$\frac{B_2}{B_2^{HS}}=\frac{1}{16\pi R_c^{9/2}W^{3/2}}\left(2\sqrt{R_cW}\left(-6D(D+2R_c)+3D\right.\right.$$

$$\times\exp\left[\frac{\pi}{2}R_cWD\right](D+4R_c)+\pi R_cW(D+2R_c)^3R_c\right)$$

$$+3\sqrt{2D}(D-\pi R_cW(D+2R_c)^2)$$

$$\left.\times\operatorname{Erf}i\left[\sqrt{\frac{\pi R_cDW}{2}}\right]\right), \tag{21}$$

where $W=W(x=0)$ and $D=D_s(\rho)$, i.e., the explicit density dependence has been suppressed for notational clarity. The imaginary error function $\operatorname{Erf}i[z]$ is defined as $\operatorname{Erf}[iz]/i$; its

values are real. As can be seen in Fig. 13, this expression compares well with the direct simulation results, demonstrating that the potential (17) is a good approximation to the true depletion potential. For this reason, we also plot the theoretical B_2 for two smaller q's. The density ρ/ρ^* at which one would expect a (metastable) critical point and a related fluid–fluid demixing decreases with decreasing q. To compare with experiments, one should keep in mind that our parameter ρ/ρ^* would be equal to the density in a reservoir of polymers kept at the same chemical potential as a full polymer–colloid mixture.[42]

If the pair-potentials are of sufficiently short range, the fluid–fluid transition becomes metastable with respect to the fluid–solid transition of the larger particles,[7,8,68] which widens significantly. It has been recently found that this generic widening of the fluid–solid transition is primarily driven by the value of the potential at contact;[2,69] other details such as the shape and range of the attractive part of the potential are less important. Roughly speaking, the fluid–solid liquidus curve widens to about half the packing fraction of the hard-sphere freezing transition when $V(0) \approx 2.5 \pm 0.5$.[2] When combined with the criterion that $B_2^* \approx -1.5$ at the critical density, this can be used for a rough prediction of the q below which the fluid–fluid transition is metastable with respect to the fluid–solid one. The minimum q for which the fluid–fluid transition is still stable is between 0.3 and 0.5, which is consistent with other calculations,[7,8,14,30] and experiments.[9,10] Of course one should keep in mind that the larger the size ratio q, the more important three-body and higher order interactions become.[30,70] These pair-potential criteria should therefore become less accurate for increasing q.

Both RG theory[34] and integral equation approaches[31,71] predict that for large enough q, B_2^* should go through a minimum as a function of ρ/ρ^*, although the two theories differ significantly on quantitative details. Experiments seem to show similar effects.[66] Remarkably, expression (21), which is based on the simple potential of Eq. (17) also shows a minimum, as shown in Fig. 14. Even more surprisingly, considering how the potential was derived, is that the minimum is near $\rho/\rho^* = 1$, as predicted by RG theory, and that it closely follows the asymptotic law $\min(B_2^*) = 1 - 0.5q^{0.401}$, derived by Eisenriegler[34] (see the inset of Fig. 14). In contrast, when the simpler Derjaguin expression (12) is used for B_2^*, no minimum as a function of ρ/ρ^* appears for large q. At present it is not clear why our expression for B_2^*, Eq. (21), should agree so well with the RG results in this large R_g/R_c regime.

V. DISCUSSION AND CONCLUSION

We have used a combination of computer simulations and theory to derive the depletion interactions induced by excluded volume polymers. Our main computer simulation results are depicted in Figs. 4 and 5 and our main theoretical results are the depletion potential for two plates, given by Eq. (4) and the depletion potential for two spheres, given by Eq. (17).
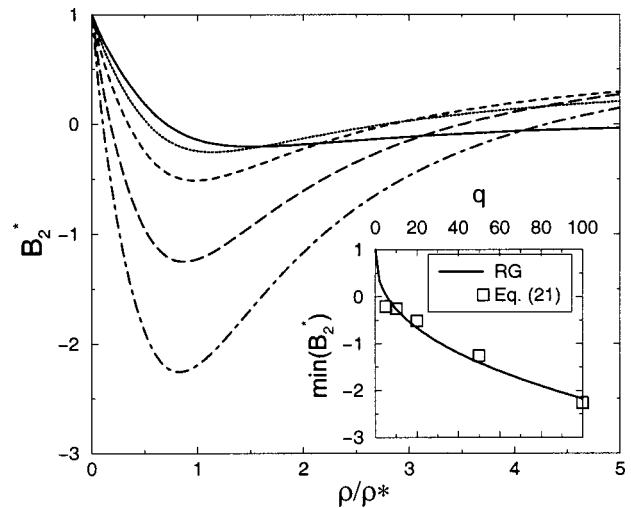
For two plates, we found that a simple linear depletion

FIG. 14. Virial coefficient from Eq. (21) as a function of polymer density for large size ratios: $q = 5$ (solid line), $q = 10$ (dotted line) $q = 20$ (dashed line), $q = 50$ (long-dashed line), and $q = 100$ (dot-dashed line). Inset: Comparison of the minimum of B_2^* as a function of q to the asymptotic RG result $\min(B_2^*) = 1 - 0.5q^{0.401}$. The agreement is remarkable.

potential (4) with a well-depth of $W(0) = -2\gamma_w(\rho)$, and a slope of $\Pi(\rho)$ is very accurate. The range decreases with density, with the largest relative change occurring in the dilute regime. In the semidilute regime, the well-depth scales as $W(0) \sim \rho^{1.539}$, while the range scales as $D_w(\rho) \sim \rho^{-0.770}$. The depletion potential also takes on a simpler functional form, given by Eq. (6). These results differ significantly from theories based on ideal polymers.

For two spheres, we find that the simple Derjaguin approximation works much better than expected due to a cancellation of errors related to the deformation of the polymers around a sphere. Interestingly, the Derjaguin expression for the force at contact seems particularly accurate, even for very large size ratios q. We used this observation, together with a correction for the Derjaguin range, to derive the depletion potential $V_s(r)$ [Eq. (17)], which was shown to agree quantitatively with our direct computer simulation results. While the excellent agreement with simulations is gratifying, further study is needed to understand why our main ansatz, that the force at contact is accurately approximated by the Derjaguin approximation, works so well for such a wide range of q.

The range of our potential scales with density in the same way that the range for the two plates does. But in contrast to the case of two plates, where the well depth at contact is more attractive than that for ideal polymers, the well depth at contact for two spheres is less attractive than that predicted by ideal polymer theories. For example, in the semidilute regime, $V_s(0) \sim -\rho^{0.770}$, compared to the scaling of the AO potential, $V_{AO}(0) \sim -\rho$. In other words, ideal polymer theories overestimate both the range *and* the well-depth of the depletion potential between two spheres, induced by interacting polymers.

We also calculated the depletion potential between spheres induced by polymers coarse-grained as "soft colloids." For the dilute regime, good agreement with the direct simulations of SAW polymers was achieved. However, for

the highest density, $\rho/\rho^* = 2.32$, the polymers as soft colloids approach strongly overestimates the depth of the depletion potential. We traced this discrepancy to a breakdown of the potential superposition approximation, something also found for two plates.[39] However, since our coarse-graining scheme is mainly useful for $q \lesssim 1$, where phase-separation sets in for $\rho/\rho^* \lesssim 1$, this breakdown at high density is not relevant to the equilibrium phase behavior of colloid–polymer systems. In fact, we have recently used this scheme to calculate the phase separation binodals of polymer–colloid mixtures for several size ratios $q \lesssim 1$.[72] Direct simulations of SAW polymers and colloids would be significantly more expensive. The advantage over directly using a pair-potential such as Eq. (17), is that many-body interactions are also effectively taken into account.[72]

Virial coefficients can provide a sensitive measure of the quality of an effective potential. We were able to integrate Eq. (17) to derive an analytical representation of the virial coefficient (21), which compares very well with the direct simulation results. Surprisingly, this same analytic form agrees quantitatively with RG results in the limit $q \gg 1$. Further study is needed to clarify why Eq. (21) works so well in this limit.

A careful comparison with experiments is complicated by the fact that most measurements are of phase behavior or structure, which depend only indirectly on the depletion interactions. The most extensive direct measurements of the depletion potential between spheres, carried out by Verma *et al.*,[16] were on a system with semiflexible polymers (DNA) which do not follow the same scaling laws as the SAW polymers we treated in this paper. However, given a good model for the equation of state and the adsorption $\hat{\Gamma}(\rho)$ for these polymers, it would be straightforward to calculate the depletion potentials using methods derived in this paper. A detailed comparison with experiments will be the subject of an upcoming review.[73]

This paper has concerned itself with the case of interacting, non-adsorbing polymers in a good solvent. By taking Eqs. (1), (2), (4), and (17) together, it follows that accurate depletion potentials can be calculated with only a knowledge of the adsorption $\hat{\Gamma}(\rho)$ and the equation of state $\Pi(\rho)$. This implies that the effect of changing solvent quality, or of adding attractions or repulsions between the colloids and the polymers can be understood by seeing how they affect these two quantities. Note that this is different from binary colloid mixtures, where the effects of added interparticle attractions and repulsions have a more subtle effect on the resultant depletion potentials.[49]

It is not hard to see that for polymers in a good solvent, adding an attractive (repulsive) polymer–colloid interaction results in a less (more) attractive depletion potential, and possibly even to repulsive effective interactions. This follows since $\Pi(\rho)$ is unchanged, and only $\hat{\Gamma}(\rho)$ is affected in an obvious way. An example where this may be relevant concerns the common practice to stabilize colloidal particles by a short polymer brush. The interaction of the free polymers with the polymer brush can be quite subtle,[74] but our theory implies that it is only the overall change in the adsorption

which effects the depletion potential, and by extension, the phase behavior.

Changing the solvent quality has a less obvious effect, since both $\Pi(\rho)$ and $\hat{\Gamma}(\rho)$ are affected. For a given density, we expect the absolute magnitudes of both to decrease, so that the strength of the depletion potential should decrease as well. Of course, for strong deviations from the case of non-adsorbing polymers in a good solvent, some of the simplifying assumptions that went into the derivation of the depletion potentials may begin to break down. For example, for very strong adsorption, the system may show bridging flocculation,[50] or gelation.[75] A rich phenomenology may be expected; this will be the subject of an upcoming investigation.[76]

ACKNOWLEDGMENTS

APPENDIX A: DERJAGUIN APPROXIMATION FOR THE ASAKURA–OOSAWA MODEL

1. Comparison for fixed parameter R_{AO}

The Asakura Oosawa model, where the ideal polymers are modeled as interpenetrable spheres of radius R_{AO}, was first introduced in 1958.[6] Between two plates this results in the linear depletion potential similar to Eq. (9), with a range R_{AO}, while between two spheres it results in the well-known Asakura–Oosawa form,

$$V_{AO}(x) = -\rho \frac{4\pi}{3}(\sigma_{cp})^3 \left\{ 1 - \frac{3}{4}\left(\frac{x+2R_c}{\sigma_{cp}}\right) \right.$$
$$\left. + \frac{1}{16}\left(\frac{x+2R_c}{\sigma_{cp}}\right)^3 \right\}, \quad 0 \leq x \leq 2R_{AO} \quad (A1)$$

which is exact within the confines of the AO model. Here we defined $\sigma_{cp} = R_c + R_{AO}$. Similarly, the use of the Derjaguin approximation (11) together with the linear AO potential between two plates results in

$$V_{AO}^{Derj}(x) = -\rho \frac{\pi}{2} R_c (2R_{AO} - x)^2, \quad 0 \leq x \leq 2R_{AO}. \quad (A2)$$

Comparison of the two expressions at contact, where $V_{AO}(0) = -\rho 2\pi (R_c R_{AO}^2 + 2R_{AO}^3/3)$ and $V_{AO}^{Derj}(0) = -\rho 2\pi \times R_c R_{AO}^2$, shows that the Derjaguin expression (A2) underestimates the well depth at contact with respect to the exact expression (A1), a discrepancy which gets relatively worse for decreasing R_c/R_{AO}. This is illustrated in Fig. 15(a) for the same size ratios we used for the interacting polymers. Since the Derjaguin approximation is only valid for large R_c/R_{AO}, this breakdown is expected.
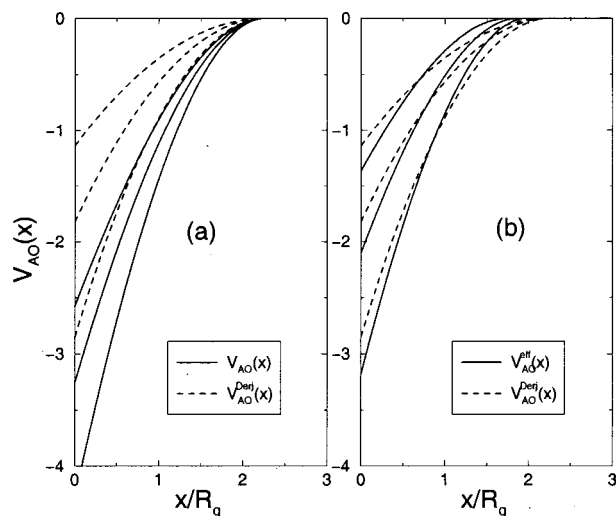
FIG. 15. (a) Comparison of the full Asakura–Oosawa model interaction (A1) with $R_{AO}=2/\sqrt{\pi}$ to the Derjaguin approximation (A2) with the same R_{AO}. The hard sphere sizes are the same as in Fig. 5. The potentials, from bottom to top, correspond to $q=1.68$, $q=1.05$, and $q=0.67$ respectively. The polymer density is $\rho/\rho^*=1$. (b) The same comparison as in (a), but now the decrease of the depletion layer range with decreasing sphere size is taken into account by using the effective AO parameter R_{AO}^{eff}, defined in Eq. (A3), in the full AO expression (A1). For the Derjaguin approximation expression $R_{AO}=2/\sqrt{\pi}$ is unchanged. The agreement is now much better.

2. Comparison with effective parameter $R_{AO}^{eff}(R_g, R_c)$

Before using the AO model to describe polymers, one needs to fix the parameter R_{AO}. A common prescription has been to take $R_{AO}=R_g$.[6] However, between two walls, one should take $R_{AO}=(2/\sqrt{\pi})R_g$, which corresponds to approximating the depletion layer of ideal polymers by a step function with the same depletion volume. This then results in a well-depth which is equal to that found for ideal polymers.[39]

However, for polymers of a given size R_g, the width of the depletion layer around a single sphere will decrease with decreasing R_c, because the polymers can partially wrap around the colloidal particles.[30,77] By equating the one-body insertion free energy for a HS sphere into a bath of AO model particles to that found for inserting a HS into a bath of ideal polymers, we found, in Paper I, an exact analytic prescription for the effective parameter R_{AO}^{eff},

$$\frac{R_{AO}^{eff}}{R_g} = \frac{1}{q}\left(\left(1+\frac{6}{\sqrt{\pi}}q+3q^2\right)^{1/3}-1\right), \qquad (A3)$$

which decreases with decreasing R_c as expected. Just because the one-body terms are equal does not mean that the same prescription for R_{AO} will work for the two-body terms, but direct computer simulations[30] have shown that using R_{AO}^{eff} in the full AO expression (A1) results in a much better approximation of the depletion potential between two spheres in a bath of ideal polymers, than using a prescription which fixes R_{AO} independently of R_c.

With this in mind, we now compare again the Derjaguin expression (A2) with $R_{AO}=2/\sqrt{\pi}R_g$ to the full AO expression (A1) but now with an effective AO radius R_{AO}^{eff} from Eq. (A3) appropriate to the desired R_c. As demonstrated in Fig. 15(b), the Derjaguin approach is now a more faithful

approximation of the full AO model depletion potential, which is itself a better approximation of the true depletion potential induced by ideal polymers. Although the Derjaguin approach does not capture the slight reduction in range, the well-depth is much closer to the AO value.

Of course, this improvement arises from a cancellation of errors. However, for the interacting polymers the depletion potential between two walls is also well described by a linear form, and we expect the same deformation effect to be relevant for polymers near spheres. Therefore, we might hope for a similar cancellation of errors when the Derjaguin expression is used for interacting polymers.

[1] C. N. Likos, Phys. Rep. **348**, 267 (2001).
[2] A. A. Louis, Philos. Trans. R. Soc. London, Ser. A **359**, 939 (2001).
[3] J. P. Hansen and I. R. McDonald, *Theory of Simple Liquids*, 2nd ed. (Academic, London, 1986).
[4] D. Frenkel and B. Smit, *Understanding Molecular Simulations* (Academic, New York, 1995).
[5] S. Asakura and F. Oosawa, J. Chem. Phys. **22**, 1255 (1954).
[6] S. Asakura and F. Oosawa, J. Polym. Sci. **33**, 183 (1958), A. Vrij, Pure Appl. Chem. **48**, 471 (1976).
[7] A. P. Gast, C. K. Hall, and W. B. Russel, J. Colloid Interface Sci. **96**, 251 (1983).
[8] H. N. W. Lekkerkerker, W. C. K. Poon, P. N. Pusey, A. Stroobants, and P. B. Warren, Europhys. Lett. **20**, 559 (1992).
[9] F. L. Calderon, J. Bibette, and J. Bais, Europhys. Lett. **23**, 653 (1993).
[10] S. M. Ilett, A. Orrock, W. C. K. Poon, and P. N. Pusey, Phys. Rev. E **51**, 1344 (1995).
[11] A. Weiss, K. D. Hörner, and M. Ballauff, J. Colloid Interface Sci. **213**, 417 (1999).
[12] A. Moussaid, W. C. K. Poon, P. N. Pusey, and M. F. Soliva, Phys. Rev. Lett. **82**, 225 (1999).
[13] A. A. Louis, R. Finken, and J. P. Hansen, Europhys. Lett. **46**, 741 (1999).
[14] M. Dijkstra, J. Brader, and R. Evans, J. Phys.: Condens. Matter **11**, 10079 (1999).
[15] Y. N. Ohshima *et al.*, Phys. Rev. Lett. **78**, 3963 (1997).
[16] R. Verma, J. C. Crocker, T. C. Lubensky, and A. G. Yodh, Phys. Rev. Lett. **81**, 4004 (1998); Macromolecules **33**, 177 (2000).
[17] C. Bechinger, D. Rudhardt, P. Leiderer, R. Roth, and S. Dietrich, Phys. Rev. Lett. **83**, 3960 (1999).
[18] J. F. Joanny, L. Leibler, and P. G. de Gennes, J. Polym. Sci., Polym. Phys. Ed. **17**, 1073 (1979).
[19] G. J. Fleer, J. M. H. M. Scheutjens, and B. Vincent, ACS Symp. Ser. **240**, 245 (1984).
[20] J. Y. Walz and A. Sharma, J. Colloid Interface Sci. **168**, 485 (1994).
[21] P. B. Warren, S. M. Ilet, and W. C. K. Poon, Phys. Rev. E **52**, 5205 (1995).
[22] R. Dickman and A. Yethiraj, J. Chem. Phys. **100**, 4683 (1994).
[23] A. Hanke, E. Eisenriegler, and S. Dietrich, Phys. Rev. E **59**, 6853 (1999).
[24] F. Schelesenger, A. Hanke, R. Klimpel, and S. Dietrich, Phys. Rev. E **63**, 041803 (2001).
[25] R. Tuinier and H. N. W. Lekkerkerker, Eur. Phys. J. E **6**, 129 (2001).
[26] R. Roth, R. Evans, and S. Dietrich, Phys. Rev. E **62**, 5360 (2000).
[27] B. Götzelmann, R. Roth, S. Dietrich, M. Dijkstra, and R. Evans, Europhys. Lett. **47**, 398 (1999); R. Roth, doctoral thesis, Bergische Universität Wuppertal, 1999.
[28] A. A. Louis and R. Roth, J. Phys.: Condens. Matter **33**, L777 (2001); R. Roth, R. Evans, and A. A. Louis, Phys. Rev. E **64**, 051202 (2001).
[29] M. Dijkstra, R. van Roij, and R. Evans, Phys. Rev. Lett. **81**, 2268 (1998); **82**, 117 (1999); Phys. Rev. E **59**, 5744 (1999).
[30] E. J. Meijer and D. Frenkel, Phys. Rev. Lett. **67**, 1110 (1991); J. Chem. Phys. **100**, 6873 (1994).
[31] M. Fuchs and K. S. Schweizer, Phys. Rev. E **64**, 021514 (2001).
[32] P. G. de Gennes, C. R. Acad. Sci. Paris. B **288**, 359 (1979).
[33] P. G. de Gennes, *Scaling Concepts in Polymer Physics* (Cornell University Press, Ithaca, 1979).
[34] E. Eisenriegler, J. Chem. Phys. **113**, 5091 (2000).

[35] A. A. Louis, P. G. Bolhuis, J. P. Hansen, and E. J. Meijer, J. Chem. Phys. **116**, 10547 (2002).

[36] M. Doi and S. F. Edwards, *The Theory of Polymer Dynamics* (Oxford University Press, Oxford, 1986).

[37] B. V. Derjaguin, Kolloid-Z. **69**, 155 (1934).

[38] A. A. Louis, P. G. Bolhuis, J. P. Hansen, and E. J. Meijer, Phys. Rev. Lett. **85**, 2522 (2000).

[39] P. G. Bolhuis, A. A. Louis, J. P. Hansen, and E. J. Meijer, J. Chem. Phys. **114**, 4296 (2001).

[40] P. G. Bolhuis, A. A. Louis, and J. P. Hansen, Phys. Rev. E **64**, 021801 (2001).

[41] P. G. Bolhuis and A. A. Louis, Macromolecules **35**, 1860 (2002).

[42] It is generally most natural to analyze depletion systems in a semigrand ensemble, where the colloidal particles are in osmotic equilibrium with a reservoir of polymers at fixed chemical potential μ (Refs. 8, 29). Throughout this paper, therefore, the polymer density ρ is actually that of a reservoir of polymers at the same chemical potential μ. For the two-particle depletion problem in the thermodynamic limit, this is equivalent to the actual polymer density, but if one wants to use the depletion potential to analyze the phase behavior of a many colloid system, this prescription should be kept in mind.

[43] Y. Mao, P. Bladon, H. N. W. Lekkerkerker, and M. E. Cates, Mol. Phys. **92**, 151 (1997).

[44] R. Maasen, E. Eisenriegler, and A. Bringer, J. Chem. Phys. **115**, 5292 (2001).

[45] It would be straightforward to generalize the potential to one with a slightly more rounded shape, such as that found for ideal polymers (Refs. 5, 39). Although this would be slightly more accurate, the differences are so small that we will stick to the simpler linear form for this paper. The definition for the range would remain the same for both versions of the potential.

[46] M. G. Noro and D. Frenkel, J. Chem. Phys. **113**, 2941 (2000).

[47] J. van der Gucht, N. A. M. Besseling, J. van Male, and M. A. Cohen Stuart, J. Chem. Phys. **113**, 2886 (2000).

[48] Y. Mao, M. E. Cates, and H. N. W. Lekkerkerker, Physica A **222**, 10 (1995).

[49] A. A. Louis, E. Allahyarov, H. Löwen, and R. Roth, cond-mat/0110385.

[50] A. Broukhno, B. Jonsson, T. Akesson, and P. N. Vorontsov-Velyaminov, J. Chem. Phys. **113**, 5493 (2000).

[51] B. Vincent, J. Edwards, S. Emmett, and R. Croot, Colloids Surf. **31**, 267 (1988).

[52] R. Tuinier and H. N. W. Lekkerkerker, Phys. Rev. E (to be published).

[53] To compare to the results of Ref. 22 we used their expression for the end-to-end distance R_e^0 for the three-dimensional fluctuating bond model, to derive the radius of gyration at zero density through $R_g = R_e^0 / \sqrt{6.06}$ (Ref. 36). The two results with the highest monomer density are not shown since they appear to be closer to the melt than to the semidilute regime.

[54] M. Triantafillou and R. D. Kamien, Phys. Rev. E **59**, 5621 (1999).

[55] R. Tuinier, G. A. Vliegenthart, and H. N. W. Lekkerkerker, J. Chem. Phys. **113**, 10768 (2000).

[56] A. A. Louis, P. G. Bolhuis, R. Finken, V. Krakoviack, E. J. Meijer, and J. P. Hansen, Physica A **306**, 251 (2002).

[57] R. L. Henderson, Phys. Lett. A **49**, 197 (1974); J. T. Chayes and L. Chayes, J. Stat. Phys. **36**, 471 (1984).

[58] L. Reatto, Philos. Mag. A **58**, 37 (1986); L. Reatto, D. Levesque, and J. J. Weis, Phys. Rev. A **33**, 3451 (1986).

[59] P. Attard, J. Chem. Phys. **91**, 3083 (1989).

[60] T. Biben, P. Bladon, and D. Frenkel, J. Phys.: Condens. Matter **8**, 10799 (1996).

[61] J. Dzubiellar and C. N. Likos, Europhys. Lett. **58**, 133 (2002); J. Chem. Phys. **116**, 9518 (2002).

[62] A. Jusufi, J. Dzubiella, C. N. Likos, C. von Ferber, and H. Löwen, J. Phys.: Condens. Matter **13**, 6177 (2001).

[63] C. N. Likos, H. Löwen, M. Watzlawek, B. Abbas, O. Jucknischke, J. Allgaier, and D. Richter, Phys. Rev. Lett. **80**, 4450 (1998); M. Watzlawek, C. N. Likos, and H. Löwen, *ibid.* **82**, 5289 (1999).

[64] S. Amokrane, J. Chem. Phys. **108**, 7459 (1998).

[65] H. De Hek and A. Vrij, J. Colloid Interface Sci. **88**, 258 (1982).

[66] A. M. Kulkarni, A. P. Chatterjee, K. S. Schweizer, and C. F. Zukoski, Phys. Rev. Lett. **83**, 4554 (1999).

[67] G. A. Vliegenthart and H. N. W. Lekkerkerker, J. Chem. Phys. **112**, 5364 (2000).

[68] M. H. Hagen and D. Frenkel, J. Chem. Phys. **101**, 4093 (1994).

[69] A. A. Louis, R. Finken, and J. P. Hansen, Phys. Rev. E **61**, R1028 (2000).

[70] D. Goulding and S. Melchionna, Phys. Rev. E **64**, 011403 (2001).

[71] A. P. Chatterjee and K. S. Schweizer, J. Chem. Phys. **109**, 10477 (1998).

[72] P. G. Bolhuis, A. A. Louis, and J. P. Hansen cond-mat/0206061 (preprint).

[73] A. A. Louis, J. Phys. Condens. Matter (in preparation).

[74] A. Jones and B. Vincent, Colloids Surf. **42**, 113 (1989).

[75] A. Johner, J. F. Joanny, S. Diez Orrite, and J. Bonet Avalos, Europhys. Lett. **56**, 549 (2001).

[76] V. Krakoviack, A. A. Louis, and J. P. Hansen (unpublished).

[77] E. Eisenriegler, A. Hanke, and S. Dietrich, Phys. Rev. E **54**, 1134 (1996).